# IPGP/CEA-LETI DGRF 2015 candidate model for IGRF-13

This note is to provide the information requested to accompany the DGRF 2015 candidate model that our IPGP-led team wishes to submit for consideration for IGRF-13.

## 1) Team

Lead Institution: Institut de Physique du Globe de Paris/Université de Paris (IPGP)
Participating Institution: CEA-LETI, Grenoble, France
Co-Team leaders: P. Vigneron (IPGP), G. Hulot (IPGP)
Team members: Jean-Michel Léger (CEA-LETI), Thomas Jager (CEA-LETI)

## 2) Data used

**Data type and version:** Only data collected by the Alpha and Bravo from the ESA Swarm mission have been used. The magnetic data are the ASM-V data produced by the ASM instruments running in vector mode (see Léger et al., 2015), processed within IPGP using L0 data version 0201, v7 version software (developed by CEA-LETI) to produce L1a data, XPa1B software to produce L1b data with UTC time stamps, using stray field corrections from 0506/0506 nominal ASMxAUX, and updated CCDB with optimized gains (1.22 for Alpha, 1.27 for Bravo, as provided by CEA-LETI on 23/04/18). These data are therefore calibrated in a slightly different way than those used in previous publications using ASM-V data (Vigneron et al., 2015; Hulot et al., 2015) to correct for artefacts that have since been identified. All the ASM-V data used are expressed in the reference frame of the ASM instruments. Attitude information is recovered using the q_NEC_CFR quaternion information from 0506/0506 MAGxLR files, also used to recover satellite positions (radius/lat/long). Note that Euler angles defining the rotation between the ASM and STR CRF reference frames are therefore jointly computed with the models (see below).

**Data temporal distribution**: First data used is from 30/11/2013, last data used is from 03/05/2019 (65 months). Note that we did not use more recent data, as this was not deemed necessary to derive a model for epoch 01/01/2015.

**Data selection:** Data selection criteria are identical (except for possible thresholds when using indices, see below) to those previously used in Hulot et al. (2015), where details can be found. These can be summarized in the following way:

- Only night-side data are used
- Magnetically quiet conditions (based on RC<2nT/h and Kp<2+) are required
- For all (absolute) QD latitudes above 55°, only scalar data have been used, also requesting that $E_{m,12}$< 0.8 mV/m
- For all other QD latitudes, only vector data have been used, unless the scalar residual (difference between scalar and modulus of vector) is larger than 0.3 nT, or the piezoelectric motor has been activated within 3s of the data measurement (since this may produce artefacts, see Léger et al., EPS, 2015), in which case only the scalar data is considered.
- A final decimation is being used to avoid over-representation along tracks (amounting to separate data by about 30s)

Again as in Hulot et al. (2015), a mild additional selection criteria was finally introduced to ensure that a meaningful (non-spurious) L1b nominal data version 0505/0506 (from the VFM instruments) was available for each ASM-V data selected, to build a mirror L1b data set for comparison purposes, which we used for assessing model uncertainties (see section 6 below).
This resulted in the selection of **313 601 scalar data** and **1 340 172 x 3 vector data**, distributed in time and latitude as illustrated in Figure 1.

## 3) Parent model parameterization:

The model parameterization used is an evolution of the one used in Hulot et al. (2015), using an approach similar to that used for the CHAOS-4 model (Olsen et al., 2014) to better account for temporal evolution over more than 5 years. It involves a grand total of **6755** coefficients corresponding to:

- Time-varying internal field up to degree and order 13 (included), using order-6 B-splines with a 6 months knots separation. This led to 16 splines and 16x13x(13+2) = **3120** coefficients

- Static internal field between degree and order 14 (included) and degree and order 45 (included). This led to and additional 45(45+2) – 13(13+2) = **1920** coefficients
- External field modelled as in Hulot et al. (2015, where details can be found):
    - Remote magnetospheric sources : $q_n^{0,GSM}$ in GSM frame, with n=1,2 -> 2 coefficients
    - Near magnetospheric ring current :
      up to degree and order 2 in SM frame -> 8 coefficients
      Δq estimated every 5 days for q10 (395 time segments, -> 395 coefficients)
      Δq estimated every 30 days for qs11 (67 time segments, -> 2x67 = 134 coefficients)

  Leading to a total of 2+8+395+134 = **539** coefficients
- Euler angles (rotation between ASM and STR reference frames) estimated every 10 days for both satellites : 197/195 time segments for Alpha and Bravo, -> 3x(197+195) = **1176** coefficients

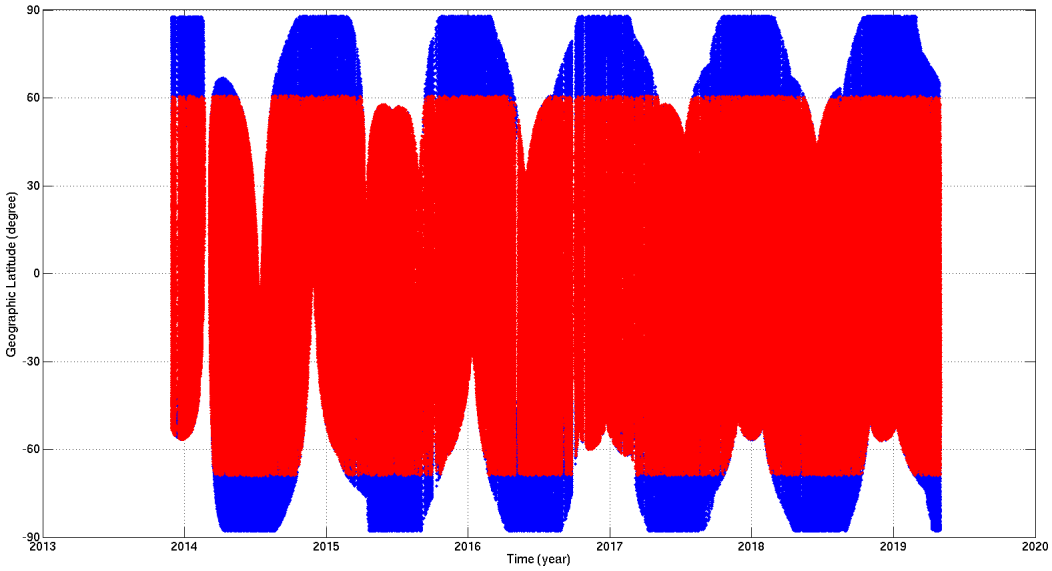


***Figure 1****: Data distribution as a function of time and latitude (blue: scalar data; red: vector data)*

**4) Parent model optimization:**

The model was computed by minimizing the mismatch between data and model prediction, using iteratively reweighted least-squares with Huber weights and temporal damping as in Olsen et al. (2014), but only using two damping parameters λ2 and λ3:

- λ2 : $|d^2B_r/dt^2|$ constrained at beginning and end of dataset (namely Nov-2013 and May-2019) with the same damping value as for CHAOS-4 (λ2 = 10)
- λ3 : $|d^3B_r/dt^3|$ integrated at the core surface and over the time coverage constrained with the same damping value as CHAOS-4 (λ3 = 0.33 for all Gauss coefficients except for $g_{10}$ where λ3=10)

As in Hulot et al. (2015), a geographical weight was introduced, proportional to sin($\theta$) (where $\theta$ is the geographic colatitude), to balance the geographical sampling of data. Anisotropic magnetic errors due to attitude uncertainty were taken into account assuming an isotropic attitude error of 10 arcsecs (recall, indeed, that even isotropic attitude error produces anisotropic magnetic errors, see Holme and Bloxham (1996), the formalism of which we rely on). A priori data error variances were otherwise set to 2.2 nT for both scalar and vector data. The starting model used is a static model (CHAOS-4 up to degree and order 13 only for epoch 30/11/13), but this choice was found to not have any influence on the final model.

A total of eight iterations were used, which was found to ensure convergence to within the accuracy required.

Resulting residual statistics are shown in Tables 1 and 2. Tables 3 and 4 provide the same statistics for the twin model produced using the Swarm L1b nominal data version 0505/0506.

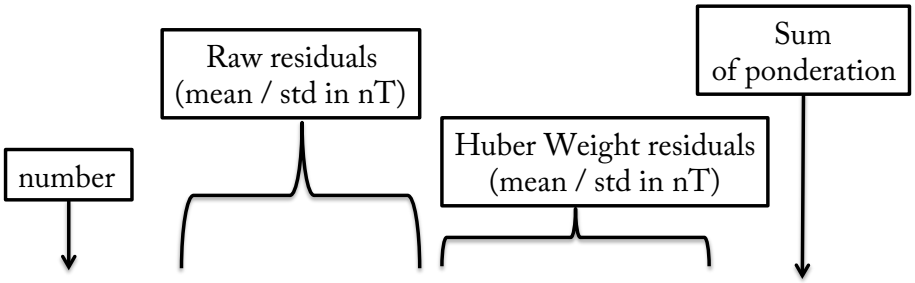


| | | | | | | | |
|---|---|---|---|---|---|---|---|
| Number F at polar latitudes: = | | 313601 | | | | | |
| F (polar) | [nT]: | 313601 | 0.67 | 7.42 | -0.07 | 3.87 | 0.84 |
| F+B_B | [nT]: | 1653773 | 0.15 | 3.95 | 0.03 | 2.55 | 0.94 |
| F+B_B low lat : | | 1340172 | 0.03 | 2.53 | 0.05 | 2.19 | 0.96 |
| B_B | [nT]: | 1340172 | 0.03 | 2.53 | 0.05 | 2.19 | 0.96 |
| B_r | [nT]: | 1340172 | -0.01 | 2.43 | -0.01 | 2.16 | 0.89 |
| B_theta | [nT]: | 1340172 | 0.04 | 4.12 | 0.06 | 3.31 | 0.90 |
| B_phi | [nT]: | 1340172 | -0.02 | 3.53 | -0.01 | 2.86 | 0.90 |

***Table 1****: Residual statistics for all data used to produce the parent model (using the same convention as in Hulot et al., 2015). B_B refers to vector residuals projected along the field direction; "Low lat" refers to data within (absolute) QD latitude 55°; F (polar) refers to scalar data above (absolute) QD latitude 55°.*

| | | | | | | | |
|---|---|---|---|---|---|---|---|
| Data set 1 (SAT-A) | | | | | | | |
| Number F at polar latitudes: = | | 157073 | | | | | |
| F (polar) | [nT]: | 157073 | 0.53 | 7.68 | -0.17 | 3.98 | 0.83 |
| F+B_B | [nT]: | 823580 | 0.11 | 4.07 | 0.01 | 2.60 | 0.93 |
| F+B_B low lat : | | 666507 | 0.02 | 2.57 | 0.05 | 2.21 | 0.77 |
| B_B | [nT]: | 666507 | 0.02 | 2.57 | 0.05 | 2.21 | 0.96 |
| B_r | [nT]: | 666507 | 0.01 | 2.51 | 0.01 | 2.23 | 0.88 |
| B_theta | [nT]: | 666507 | 0.02 | 4.14 | 0.03 | 3.34 | 0.90 |
| B_phi | [nT]: | 666507 | -0.01 | 3.54 | -0.01 | 2.88 | 0.89 |
| Data set 2 (SAT-B) | | | | | | | |
| Number F at polar latitudes: = | | 156528 | | | | | |
| F (polar) | [nT]: | 156528 | 0.82 | 7.15 | 0.03 | 3.75 | 0.84 |
| F+B_B | [nT]: | 830193 | 0.18 | 3.83 | 0.05 | 2.51 | 0.94 |
| F+B_B low lat : | | 673665 | 0.03 | 2.49 | 0.06 | 2.17 | 0.78 |
| B_B | [nT]: | 673665 | 0.03 | 2.49 | 0.06 | 2.17 | 0.96 |
| B_r | [nT]: | 673665 | -0.04 | 2.34 | -0.04 | 2.08 | 0.89 |
| B_theta | [nT]: | 673665 | 0.06 | 4.11 | 0.09 | 3.29 | 0.90 |
| B_phi | [nT]: | 673665 | -0.04 | 3.52 | -0.01 | 2.84 | 0.90 |

***Table 2****: Separate Residual statistics for all Swarm Alpha (SAT-A, top Table) and Swarm Beta (SAT-B, bottom Table) data used to produce the parent model.*

| | | | | | | | |
|---|---|---|---|---|---|---|---|
| Number F at polar latitudes: = | | 313601 | | | | | |
| F (polar) | [nT]: | 313601 | 0.67 | 7.43 | -0.07 | 3.87 | 0.83 |
| F+B_B | [nT]: | 1653773 | 0.13 | 3.94 | 0.01 | 2.53 | 0.94 |
| F+B_B low lat : | | 1340172 | 0.00 | 2.49 | 0.03 | 2.16 | 0.96 |
| B_B | [nT]: | 1340172 | 0.00 | 2.49 | 0.03 | 2.16 | 0.96 |
| B_r | [nT]: | 1340172 | -0.02 | 1.74 | -0.01 | 1.55 | 0.93 |
| B_theta | [nT]: | 1340172 | -0.01 | 3.61 | 0.02 | 2.92 | 0.93 |
| B_phi | [nT]: | 1340172 | -0.02 | 3.07 | 0.01 | 2.48 | 0.92 |

***Table 3****: same as Table 1, but for the twin model produced using the Swarm L1b nominal data version 0505/0506.*

```
Data set  1 (SAT-A)
Number F at polar latitudes: = 157073
F (polar) [nT]:     157073      0.50      7.70    -0.18      4.00      0.82
F+B_B     [nT]:     823580      0.10      4.06    -0.01      2.59      0.93
F+B_B low lat :     666507      0.00      2.54     0.03      2.19      0.78
B_B       [nT]:     666507      0.00      2.54     0.03      2.19      0.96
B_r       [nT]:     666507      0.01      1.77     0.01      1.58      0.93
B_theta   [nT]:     666507      0.00      3.61     0.03      2.93      0.93
B_phi     [nT]:     666507     -0.04      3.07    -0.00      2.48      0.92

Data set  2 (SAT-B)
Number F at polar latitudes: = 156528
F (polar) [nT]:     156528      0.83      7.16     0.04      3.75      0.84
F+B_B     [nT]:     830193      0.16      3.81     0.03      2.48      0.94
F+B_B low lat :     673665      0.00      2.45     0.03      2.13      0.78
B_B       [nT]:     673665      0.00      2.45     0.03      2.13      0.96
B_r       [nT]:     673665     -0.05      1.72    -0.04      1.51      0.92
B_theta   [nT]:     673665     -0.03      3.61     0.01      2.91      0.93
B_phi     [nT]:     673665     -0.01      3.07     0.02      2.49      0.93
```

***Table 4:*** *same as Table 2, but for the twin model produced using the Swarm L1b nominal data version 0505/0506.*

### 5) DGRF 2015 candidate model generation

The DGRF 2015 candidate model is just the parent model computed for epoch 2015.0 and truncated at degree 13.

### 6) Computation of realistic uncertainties on each Gauss coefficient

To assess "realistic" uncertainties on each Gauss coefficients, we decided to only assess uncertainties produced by the quality of the data (i.e., we did not assess the uncertainties due to the choice of the modelling strategy, choice of data selection criteria and choice of parameters for the inversion, such as damping parameters, etc…). These uncertainties should thus be viewed as a lower bound indication of the "real" uncertainties.

The following strategy was used. We first split the ASM-V data set in two: ordering and numbering data as a function of time, every even number data is put in sub-dataset ASMV-1, every odd data is put in sub-dataset ASMV-2. Likewise, the twin VFM data set (Swarm L1b nominal data, version 0505/0506) is split in two VFM-1 and VFM-2 datasets (the time distribution of VFM-1/2 data matching that of ASMV-1/2). A model is next computed from each sub-dataset, using the same parameters as the parent (and twin) model, leading to four models: ASMV-1 and VFM-1 (sharing the same even number data distribution) and ASMV_2 and VFM_2 (sharing the same odd number data distribution). For each Gauss coefficients, the values A1 (from ASMV_1), A2 (from ASMV-2), V1 (from VFM1) and V2 (from VFM2) are next used to compute the quantity E = sqrt [ 1/2 x {(A1-V2)x(A1-V2) + (A2-V1)x(A2-V1)}], which we assign as one sigma type of error on the corresponding Gauss coefficient. These values are provided as s_g (for the g coefficient) and s_h (for the h coefficient) with 3 significant digits.

Note that this technique only provides estimate of variances and ignores possible cross-correlations in errors between Gauss coefficients. But it can also be used to compute the geographical distribution of the errors (one sigma type) predicted for local quantities, such as Br values (now using local values of the predicted Br by the same four models, using the same formula E = sqrt [ 1/2 x {(A1-V2)x(A1-V2) + (A2-V1)x(A2-V1)}]. Figure 2 provides a map of this predicted error.

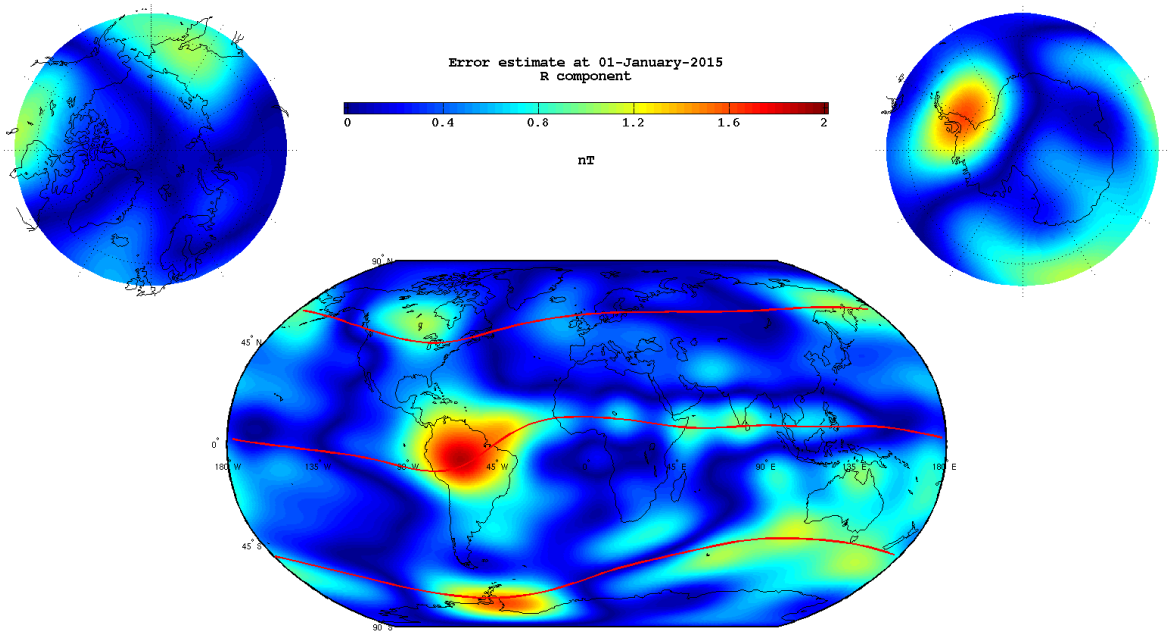


*Figure 2: Local errors (one sigma type) computed using the technique described in the text for the Br (radial component) at Earth's surface.*

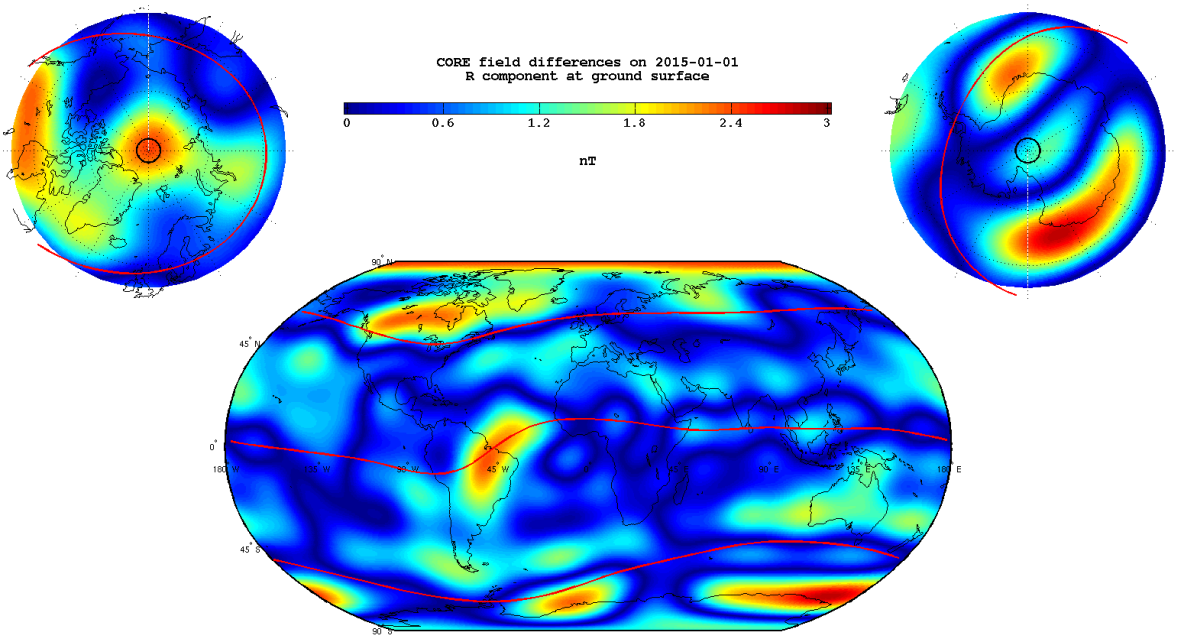


*Figure 3: Absolute value of the difference in the Br values predicted by our DGRF 2015 candidate model and CHAOS6-x9 at Earth's surface.*

## 7) Initial Validation

To provide an initial assessment of the quality of the DGRF 2015 candidate model we produced, we simply compared this model to the CHAOS6-x9 model for epoch 2015.0. This CHAOS6-x9 model was computed by DTU only using L1b Swarm data (plus data from earlier missions as well as data from ground observatories). The modelling is similar in spirit (also using splines, etc…), but differs in many details (choice of parameters, etc…), and also involves the use of gradient data (see Finlay et al., 2016). Figure 3 illustrates the geographical distribution of the absolute value of the difference in the Br values predicted by our DGRF 2015 candidate model and CHAOS6-x9. It is interesting to see that these differences have many similarities with the errors predicted by the technique described in section 6 (and shown in Figure

2) and are very comparable in magnitude, lending some credit to the estimate of uncertainties we provide for each Gauss coefficient.

We also computed the Lowes-Mauersberger spectra of the differences between our DGRF 2015 candidate model and the "twin" model computed using the VFM data (Swarm L1b nominal data version 0505/0506), as well as those of the differences of these models and previous models computed from earlier ASM-V data (the IGRF 2015 candidate model of Vigneron et al., 2015, and the more advanced model of Hulot et al., 2015) with respect to the CHAOS6-x9 model for the same epoch. These spectra are shown in Figure 4.

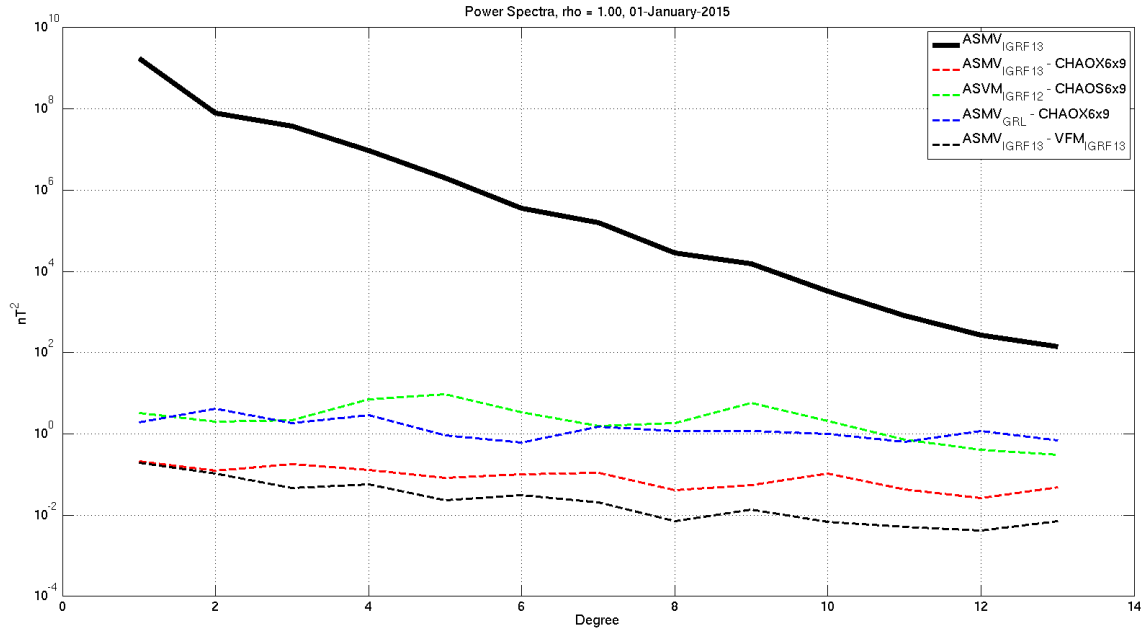


***Figure 4**: Spectra of our DGRF 2015 candidate model (black solid line, referred to as $ASMV_{IGRF\ 13}$), of the difference between our DGRF 2015 candidate model and the "twin" model computed from VFM Swarm L1b nominal data version 0505/0506 data (black dashed line, referred to as $ASMV_{IGRF\ 13}$ - $VFM_{IGRF\ 13}$), of the difference between our DGRF 2015 candidate model and CHAOS6-x9 (red dashed line, referred to as $ASMV_{IGRF\ 13}$ - CHAOS6x9), of the difference between the ASMV model published in Hulot et al. (2015) and CHAOS6-x9 (blue dashed line, referred to as $ASMV_{GRL}$ - CHAOS6x9), of the difference between the ASMV IGRF 2015 candidate model published in Vigneron et al. (2015) and CHAOS6-x9 (green dashed line, referred to as $ASMV_{IGRF\ 12}$ - CHAOS6x9), all at Earth's surface.*

Figure 4 illustrates a number of important points. One is the progressive improvement when considering the ASMV IGRF 2015 candidate model of Vigneron et al (2015), which relied on Swarm Alpha and Bravo ASM-V data before recalibration only covering the November 29, 2013 to September 25, 2014 time period using a linear SV extrapolation to 2015.0), the improved ASMV model of Hulot et al. (2015, which involved a more advanced modelling and relied on Swarm Alpha and Bravo ASM-V data before recalibration covering the November 29, 2013 to November 6, 2014 time period using a much sorter a linear SV extrapolation to 2015.0), and our DGRF 2015 candidate model, which is the closest to CHAOS6-x9, with a typical spectral disagreement of $10^{-1}nT^2$ at all degrees, consistent with the disagreement illustrated in Figure 3 (with a maximum below 3 nT). Another encouraging point worth stressing is that the disagreement between our DGRF 2015 candidate model and its "twin" model (computed from VFM Swarm L1b nominal data version 0505/0506 data) is even better, showing that the disagreement between our DGRF 2015 candidate model and CHAOS6-x9 is more due to the difference in the modelling strategy, than to differences in the ASM-V and VFM data sets. Finally, we note that the difference between our DGRF 2015 candidate model and CHAOS6-x9 is well on the very low side of the typical differences that were observed between the various DGRF 2010 candidate models and the finally adopted DRGF 2010 model, as illustrated in Figure 1 of Thébault et al. (2015).

## 8) Conclusion

We therefore conclude that our DGRF 2015 candidate model entirely based on ASM-V experimental vector mode data is a particularly valuable candidate for contribution to the final DGRF 2015 model.

**9) References:**


Finlay, C.C., Olsen, N., Kotsiaros, S., Gillet, N., Tøffner-Clausen, L., Recent geomagnetic secular variation from *Swarm* and ground observatories as estimated in the CHAOS-6 geomagnetic field model, *Earth Planets Space,* 68 : 112, https://doi.org/10.1186/s40623-016-0486-1, 2016. For the CHAOS-6-x9 version of this model, see http://www.spacecenter.dk/files/magnetic-models/CHAOS-6/.

Holme, R., and J. Bloxham, The treatment of attitude errors in satellite geomagnetic data, *Phys. Earth Planet. Inter.*, *98*, 221–233, 1996.

Hulot, G., Vigneron, P., Léger, J.-M., Fratter, I., Olsen, N., Jager, T., Bertrand, F., Brocco, L., Sirol, O., Lalanne, X., Boness, A., Cattin, V., Swarm's absolute magnetometer experimental vector mode, an innovative capability for space magnetometry, *Geophys. Res. Lett.*, 42, https://doi.org/10.1002/2014GL062700, 2015.

Léger, J.M., Jager, T., Bertrand, F., Hulot G., Brocco, L., Vigneron, P., Lalanne, X., Chulliat, A., Fratter, I., In-flight performance of the Absolute Scalar Magnetometer vector mode on board the Swarm satellites, *Earth Planets Space,* 67 : 57, https://doi.org/10.1186/s40623-015-0231-1, 2015.

Olsen, N., H. Lühr, C. C. Finlay, T. J. Sabaka, I. Michaelis, J. Rauberg, and L. Tøffner-Clausen, The CHAOS-4 geomagnetic field model, *Geophys. J. Int.*, *197*, 815–827, 2014.

Thébault E., Finlay C.C., Alken P., Beggan C.D., Canet E., Chulliat A., Langlais B., Lesur V., Lowes F.J., Manoj C., Rother M., Schachtschneider R., Evaluation of candidate geomagnetic field models for IGRF-12. Earth Planets Space, 67 : 112, https://doi.org/10.1186/s40623-015-0273-4, 2015.

Vigneron, P., Hulot, G., Olsen, N., Léger, J.M., Jager, T., Brocco, L., Sirol, O., Coïsson, P., Lalanne, X., Chulliat, A., Bertrand, F., Boness, A., Fratter, I., A 2015 International Geomagnetic Reference Field (IGRF) Candidate Model Based on *Swarm*'s Experimental Absolute Magnetometer Vector Mode Data, *Earth Planets Space,* 67 : 95, https://doi.org/10.1186/s40623-015-0265-4, 2015.